View metadata, citation and similar papers at core.ac.uk
brought to you by CORE
provided by National Chung Hsing University Institutional Repository

JOURNAL OF APPLIED PHYSICS 115, 17B715 (2014)

MoC intermediate layer for FePt magnetic recording media

Jai-Lin Tsai,[a] Qi-Shao Luo, Po-Ran Chen, and Yi-Hsiu Chen
Department of Materials Science and Engineering, National Chung Hsing University, Taichung 402, Taiwan

(Presented 6 November 2013; received 13 September 2013; accepted 28 October 2013; published online 28 January 2014)

A (001) textured FePt film was deposited on MoC/CrRu/glass at a substrate temperature of 380 °C by using magnetron sputtering. The MoC conductive intermediate layer was used to resist the Cr diffusion up to high deposition temperatures and promotes the epitaxial growth of the (001) textured FePt film. The FePt film showed high perpendicular magnetization and the out-of-plane coercivity increased with MoC thickness. The FePt/MoC (5 nm)/CrRu film showed a square out-of-plane magnetic hysteresis loop with a coercivity of 6.0 kOe and a linear-like in-plane loop. A multi-functional MoC intermediate layer exhibited heteroepitaxial relation with FePt and CrRu and was capable of resisting the interlayer diffusion at high deposition temperatures. © *2014 AIP Publishing LLC*. [http://dx.doi.org/10.1063/1.4863376]

I. INTRODUCTION

$L1_0$ FePt films have attracted considerable attention in field of heat-assisted perpendicular magnetic recordings because of high magnetocrystalline anisotropy (K_u) and the high-temperature gradient of K_u.[1–8] Reducing the ordering temperature, controlling the c-axis alignment perpendicular to the film surface with narrow switching field distribution, a granular structure with suitable segregant such as B, C, B_4C, transition-oxide and smaller grain size with columnar growth are required in FePt media.[9–17] Epitaxial growth of FePt on a suitable intermediate layer and underlayer are more effective in reducing the ordering temperature. Strain induced ordering derives from a lattice mismatch between FePt and the intermediate layer or underlayer during high temperature deposition. The non conductive MgO underlayer is deposited using RF sputtering and a low deposition temperature, a process that has been discussed extensively.[13–17] In epitaxial CrRu/FePt system, a diffusion barrier layer consisting of a material such as Pt, MgO, TiC, TiN is required.[11,18,19] In this study, a conductive MoC diffusion barrier was used between the CrRu and FePt layers. Molybdenum-carbide is a potential diffusion barrier because of its high melting point, high thermal expansion coefficient, and low bulk resistivity.[20] The MoC film with face centered cubic NaCl structure shows lattice constant around 0.427 nm and the $d_{(200)}$ spacing is 0.2135 nm. It is expected to have heteroepitaxially relationship with FePt (001)/[100] and Cr(200)/[110]. The MoC with NaCl structure shows large theoretical cohesive energy which explains large value of experimental heat of formation energy.[21] The bonding in NaCl structure MoC is composed of metallic d-binding and covalent p-d hybridization.[21] The MoC phase is formed at equal atomic ratio or higher C concentration. When the atomic concentration of C is above 50%, the MoC and C phases are co-existed. The excess C may also use as the segregant to diffuse up to separate FePt grains from intermediate layer. In this study, the MoC diffusion barrier or intermediate layer performed two functions: promoting the epitaxial growth of the (001) textured FePt film and avoiding the Cr diffusion from the underlayer to the FePt layer. The conductive MoC compound is another option (instead of the insulated MgO intermediate layer) for improving the columnar grain growth and thermal sinking after writing.

II. EXPERIMENTS

The FePt thin films with a layer structure of FePt(10 nm)/MoC(t)/CrRu(80 nm)/glass (t=0, 1, 2, 3, 4, 5 nm) were all prepared using direct current (dc) magnetron sputtering with a working pressure of 1.5×10^{-3} Torr. The CrRu layer with a thickness of 80 nm was co-sputtered on bare glass at 200 °C by using Cr and Ru element targets. The composition of CrRu films was $Cr_{82}Ru_{18}$ estimated from the total deposition time using the calibrated deposition rates for a given sputtering power. After deposition, the substrate temperature was raised to 380 °C and the MoC intermediate layer or diffusion barrier layer was prepared using $Mo_{50}C_{50}$ alloy target with thicknesses from 1 to 5 nm. The $Fe_{54}Pt_{46}$ alloy target was used and the FePt film with a thickness of 10 nm was also deposited at 380 °C.

III. RESULTS AND DISCUSSION

Figure 1 shows the XRD patterns of the FePt/MoC(t)/CrRu films with MoC diffusion barrier layers of various thicknesses (t = 0, 1, 2, 3, 4, 5 nm). The Cr (200) peak from the underlayer is clearly observed. The Ru was added to stabilize the Cr (200) and avoids the appearance of a (110) peak. The lattice constant (a) of the $Cr_{82}Ru_{18}$ film was expended to 0.290 nm as compared with that of Cr (0.288 nm) and the epitaxial relationship was $\sqrt{2}$a. The formation mechanism of the (200) textured Cr on glass substrate based on surface energy and interface energy has been theoretically demonstrated using the Winterbottom model, which was related to slowing down the nucleation and growth rate and maintaining the extensive island structure during high temperature deposition.[22] Figure 1(a) shows the

[a]Author to whom correspondence should be addressed. Electronic mail: tsaijl@dragon.nchu.edu.tw. Fax: 886-4-22857017.

 © 2014 AIP Publishing LLC

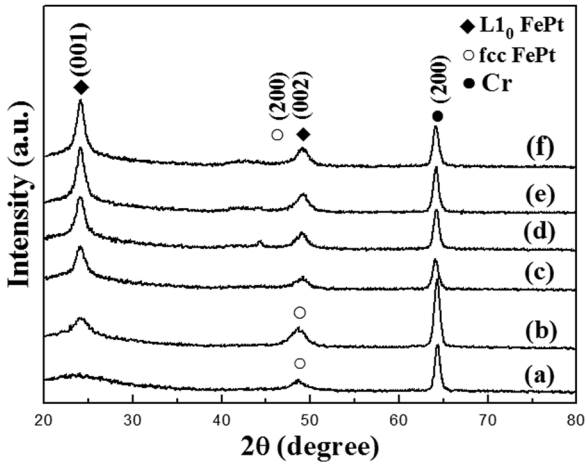

FIG. 1. Standard XRD patterns of FePt/MoC(t nm)/CrRu films, t = (a) 0, (b) 1, (c) 2, (d) 3, (e) 4, and (f) 5.

XRD pattern of the FePt/CrRu film deposited at 380 °C without an MoC barrier. The disordered face center cubic (fcc) FePt (200) peak was indexed. The disordered fcc FePt phase shows a soft magnetic property. The ordering of the FePt was deteriorated because of the Cr diffusion at a high deposition temperature of 380 °C. Figure 1(b) shows the XRD pattern of the FePt/MoC(1 nm)/CrRu film. The (001) superlattice peak is weak and broad, which indicates fewer (001) oriented FePt grains and the fcc FePt (200) peak at 48.5° was dominated. In Figs. 1(c)–1(f), the (001) superlattice diffraction peak and the (002) fundamental reflection of the L1$_0$ FePt are clearly observed and suggesting that the L1$_0$ FePt crystal has a (001) preferred orientation. When the ordering degree increased, the fcc FePt (200) was shift to higher angel at 49.2° and the L1$_0$ FePt (002) was indexed. The fcc FePt (200) and L1$_0$ FePt (002) phases are coexistence in partial ordered films. The integrated intensity of L1$_0$ FePt (001) peak increased with the thickness of MoC layer. The rocking curves of FePt (001) peak in Fig. 1(f) was measured, the value of $\Delta\theta_{50}$ which indicates full-width -at-half--maximum (FWHM) is 11.5°. The Cr (200)/[110] and MoC (200)/[100] peak along with the FePt (001)/[100] peak suggested that the heteroepitaxial relationship between the textured L1$_0$ FePt, intermediate MoC layer, and CrRu underlayer. The MoC (200) peak was not observed with thickness of 1 nm to 5 nm but appeared when the thickness of the MoC increased to 20 nm (Supplementary Fig. S1).[25] The MoC compound can be used as both the diffusion barrier and epitaxial layer. The typical ordering parameter of bulk, thick film without crystalline texture can be estimated from $[(I_{(001)}/I_{(002)})/(I^*_{(001)}/I^*_{(002)})]^{1/2}$.[23,24] For (001) textured FePt thin film, the Lorentz and absorption factors were further corrected and the theoretical ratio of FePt (001) superlattice peak to (002) fundamental peak was estimated as functions of FWHM and thickness from FePt film.[24] In Fig. 1(f), the estimated value of peak ratio (001)/(002) is 3.48 when the thickness of FePt is 10 nm. Highly textured FePt film shows lower peak ratio with the same film thickness.[24]

Figure 2 shows the out-of-plane and in-plane magnetic hysteresis loops of FePt/MoC(t)/CrRu films (t = 0, 1, 2, 3, 4, 5 nm) films. For the FePt/CrRu film without MoC diffusion barrier as shown in Fig. 2(a), the disordered FePt film was magnetic soft with in-plane magnetic anisotropy. The in-plane and out-of-plane H_c were 0.12 and 0.43 kOe, respectively. In Fig. 2(b), the FePt/MoC(1 nm)/CrRu film also shows soft magnetic properties and the in-plane and out-of-plane H_c are 0.42 and 0.52 kOe, respectively. It is suggested that the fcc

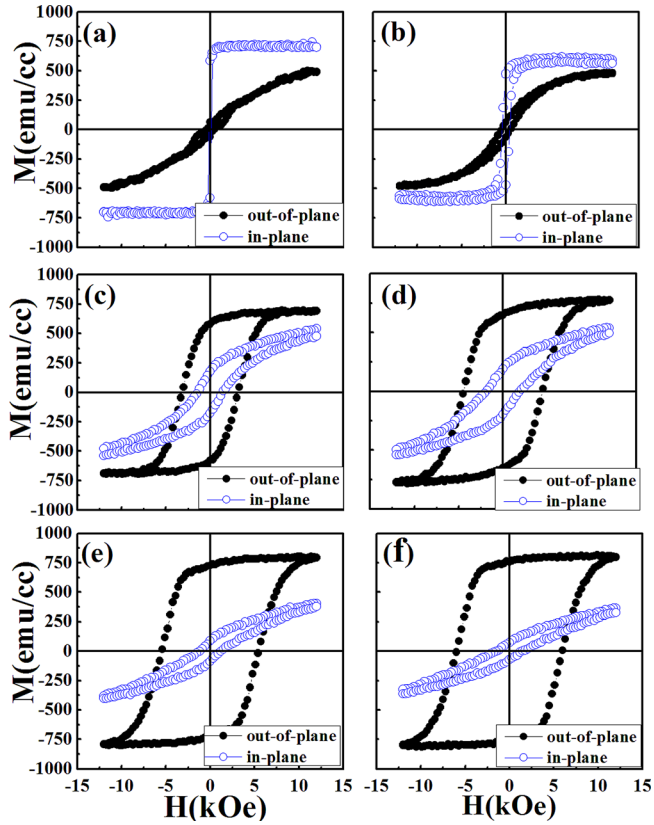

FIG. 2. Magnetic hysteresis loops of FePt/MoC(t nm)/CrRu films, t = (a) 0, (b) 1, (c) 2, (d) 3, (e) 4, and (f) 5.

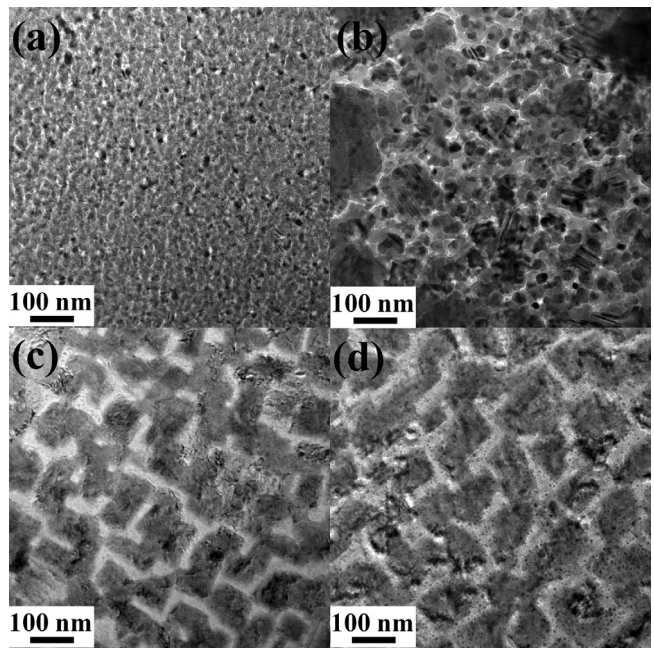

FIG. 3. TEM images of FePt/MoC(t nm)/CrRu films, t = (a) 0, (b) 2, (c) 4, and (d) 5.

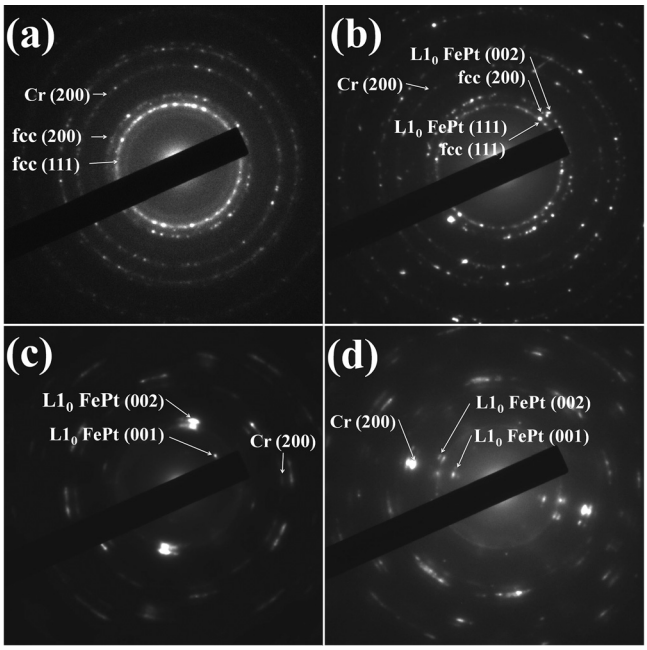

FIG. 4. Selected area diffraction patterns of FePt/MoC(t nm)/CrRu films, t = (a) 0, (b) 2, (c) 4, and (d) 5.

FePt (200) phase was dominated in Fig. 1(b) and shows soft magnetic properties in Fig. 2(b). When the thickness of the MoC layer increased to 2 nm, the FePt film was magnetic hard and characterized by perpendicular magnetization as presented in Fig. 2(c). The out-of-plane loop shows a square-like shape with H_c value of 3.2 kOe and the immense in-plane loops were caused by the lower ordering degree. Figs. 2(d)–2(f) show the loops of the FePt/MoC(t)/CrRu films (t = 3, 4, and 5 nm), the square magnetization curve and the greater out-of-plane H_c values of 4.4, 5.5, and 6.0 kOe were obtained. In addition, the areas in in-plane loops became smaller. In summary, the ordering degree and (001) texturing of the FePt film increased as the thickness of the MoC diffusion barrier increased at certain deposition temperatures.

Figures 3 and 4 show the plane-view TEM images and the selected area diffraction (SAD) patterns of the FePt/MoC(t)/CrRu films (t = 0, 2, 4, 5 nm), respectively. Figure 3(a) shows the bright field image of the FePt/CrRu film without MoC diffusion barrier. The smaller FePt grains were observed and some grains were separated by the diffused Cr from the underlayer. From the ring pattern in Fig. 4(a), the disordered fcc FePt (200) and Cr (200) planes were indexed. Figure 3(b) show the image of FePt/MoC(2 nm)/CrRu film. The FePt grains were distributed randomly and the dark background may come from MoC/CrRu grains. From the selected area diffraction pattern in Fig. 4(b), the nearly overlapped fcc FePt (200) and $L1_0$ FePt (002) rings were indexed. The clear spots and continuous pattern were all observed in FePt (111) ring and suggested that the fcc and $L1_0$ phases were coexistence. The Cr (200) planes were also indexed. Figures 3(c) and 3(d) show the bright field image of the FePt/MoC(4, 5 nm)/CrRu films. TEM investigation and energy dispersive x-ray (EDX) were performed in Fig. 3(d) to analyze the grains distributions of CrRu, MoC, and FePt (Supplementary Fig. S2).[25] The element mapping was given by HAADF (high angle angular dark field) analysis which provided atomic number (Z) dependent contrast. The distributions of CrRu, MoC, and FePt phases were mapped in Z-contrast images of FePt/MoC/CrRu film. The CrRu and MoC grains were dispersive continuous in the film. From elements mapping, almost FePt grains were concentrated in the rectangular structure area that shows specific orientation. The selected area diffraction patterns were changed from a continuous ring to arc-like ring patterns as shown in Figs. 4(c) and 4(d). The $L1_0$ FePt (002) and Cr (200) planes were indexed.

IV. CONCLUSIONS

The (001) oriented FePt film was prepared on MoC/CrRu/glass substrate. The FePt film showed higher perpendicular magnetization when the thickness of the MoC layer increased up to 5 nm. The MoC intermediate layer has multiple functions that were used to promote the epitaxial growth of (001) textured FePt to prevent the deterioration of perpendicular magnetic anisotropy because of Cr diffusion particular at high deposition temperatures and to separate the FePt grains partially from below.

ACKNOWLEDGMENTS

The authors would like to thank the National Science Council, Taiwan, for financial support under Grant No. NSC 102-2221-E-005-025. We also thank the Center of Nanoscience and Nanotechnology in NCHU for TEM investigations.

[1]D. Weller *et al.*, IEEE. Trans. Magn. **36**, 10 (2000).
[2]M. H. Hong *et al.*, J. Appl. Phys. **84**, 4403 (1998).
[3]S. N. Piramanayagam, J. Appl. Phys. **102**, 011301 (2007).
[4]H. J. Richter, J. Phys. D: Appl. Phys. **40**, R149 (2007).
[5]T. Suzuki *et al.*, IEEE. Trans. Magn. **41**, 555 (2005).
[6]T. Shima *et al.*, Appl. Phys. Lett. **88**, 063117 (2006).
[7]J. P. Liu *et al.*, Appl. Phys. Lett. **72**, 483 (1998).
[8]J. L. Tsai *et al.*, Appl. Phys. Lett. **96**, 032505 (2010).
[9]Y. F. Ding *et al.*, Appl. Phys. Lett. **93**, 032506 (2008).
[10]J. S. Chen *et al.*, J. Appl. Phys. **105**, 07B702 (2009).
[11]K. F. Dong *et al.*, J. Appl. Phys. **111**, 07A308 (2012).
[12]J. L. Tsai *et al.*, J. Appl. Phys. **111**, 07A709 (2012).
[13]L. Zhang *et al.*, J. Magn. Magn. Mater. **322**, 2658 (2010).
[14]O. Mosendz *et al.*, J. Appl. Phys. **111**, 07B729 (2012).
[15]S. D. Granz *et al.*, J. Appl. Phys. **111**, 07B709 (2012).
[16]E. Yang *et al.*, J. Appl. Phys. **111**, 07B720 (2012).
[17]J. L. Tsai *et al.*, J. Alloys Compd. **579**, 12 (2013).
[18]J. S. Chen *et al.*, Appl. Phys. Lett. **81**, 1848 (2002).
[19]J. S. Chen *et al.*, Appl. Phys. Lett. **90**, 042508 (2007).
[20]C. C. Tripathi *et al.*, Appl. Surf. Sci. **255**, 3518 (2009).
[21]H. W. Hugosson *et al.*, Chem. Phys. Lett. **333**, 444 (2001).
[22]Y. C. Feng *et al.*, J. Appl. Phys. **76**, 7311 (1994).
[23]S. D. Granz and M. H. Kryder, J. Magn. Magn. Mater. **324**, 287 (2012).
[24]E. Yang *et al.*, IEEE. Trans. Magn. **48**, 7 (2012).
[25]See supplementary material at http://dx.doi.org/10.1063/1.4863376 for Figure S1 shows the XRD diffraction patterns of FePt(380 °C)/MoC(t)/CrRu (200 °C), t = (a) 5 nm deposited at 380 °C, (b) 7 nm deposited at 380 °C, and (c) 20 nm, deposited at 200 °C and Figure S2 shows the elements mapping of FePt/MoC(5 nm)/CrRu film using EDX attached on TEM.